Observations of particle layers levitated in a radio-frequency sputtering plasma

G. Praburam[a] and J. Goree[b]
Department of Physics and Astronomy, The University of Iowa, Iowa City, Iowa 52242

(Received 25 January 1994; accepted 25 June 1994)

Submicron carbon particles are grown in an argon radio-frequency (rf) sputtering plasma with graphite electrodes. *In situ* laser light scattering revealed particles levitated in the plasma in stratified layers, which were often thinner than 0.5 mm. Under some conditions, the number of layers was very large. These layers are grouped into clouds. In a pure argon plasma, there is one cloud near the sheath edge above the lower electrode, while adding SF_6 results in additional particle clouds near the upper electrode and in the glow region. The different layers appear to separate particles according to size, with the heaviest in the lowest layer. During several hours of plasma operation, the layers collapsed and grew again into more stratified layers. The influence of parameters, such as gas pressure, rf power, electrode separation, and gas mixture was investigated. Scanning electron microscopy revealed that the particles were multisized spheres with a cauliflowerlike surface. Some of the particles were found to be coagulated, due to collisions within the plasma.

I. INTRODUCTION

Particles generated in processing plasmas are a serious problem because they degrade the quality of deposited films and they contaminate wafers. Spears *et al.*[1] demonstrated that a silane deposition plasma can grow particles, which are suspended in the plasma in a localized spatial distribution. The particles can be detected by laser light scattering (LLS). Recently, plasma-generated particles have been observed in many types of plasma processes, including deposition, sputtering, and etching.[2–6] Particles range in size from a few nanometers to tens of microns.

Particles can be trapped in the plasma by a combination of electrical, collisional, and gravitational forces. The trap is localized both vertically and laterally. In the vertical direction, particles usually reside near the sheath edge. In the lateral direction, the trap is often localized in a circular disk above an electrode.[3,5] When the plasma is turned off, the electrical maintenance of the trap ceases. The particles then fall to a surface, and they may deposit on a wafer, and contaminate it.

Trapping happens because a particle immersed in a plasma acquires a negative electrical charge by collecting electrons and ions. Since the sheath electric field has a polarity that repels negative charges from the electrodes, the particles can be levitated. Gravity and collisional drag forces provide the counter balancing forces. Particles will be trapped unless the combined effect of all these forces drives the particles to the electrode or causes them to escape in the radial direction.

Controlling particle contamination requires an understanding of the trapping, and this calls for study of the spatial distribution of the particles in the plasma. Studies of this kind have been reported by a number of experimenters who have used light scattering to observe the particles and their distribution.[4,5,7–11] Among them were Selwyn *et al.*,[5] who observed powder levitated in a radio-frequency (rf) etching reactor, and Jellum *et al.*,[7] who investigated the role of thermophoretic forces on carbon particles in an argon discharge. Silane plasmas have been used in a large number of particle experiments reported in the literature.[2,3,6,10]

Aside from the concern of particle contamination during plasma processing of surfaces, there are several other research areas where there is interest in plasma-generated particles. These include laboratory simulations of dust in the solar system,[12] and synthesis of ceramics, nanocrystalline powder, and nanocomposite materials.[13,14]

In this article, we report observations of the spatial distribution of particles grown in a parallel-plate sputtering discharge, using graphite electrodes and 13.6-MHz capacitively coupled rf power. Particles grew due to sputtering of the graphite electrode, and they were suspended in the plasma. We used LLS to observe the growth dynamics of the particles *in situ* and scanning electron microscopy to characterize the particle size and morphology *ex situ*.

Under some plasma conditions, the particles in an argon glow were found suspended in many stratified layers near the edge of the sheath at the lower electrode. Adding SF_6 increased the number of layers at the lower electrode. Also, additional layers appeared near the upper electrode and in the central glow region. To our knowledge, this is the first report of particles stratifying into a large number of layers. This observation was possible because of the high-spatial resolution of our optical setup. Previous experimenters, such as Jellum *et al.*,[7] have reported one layer at the lower electrode and sometimes one layer at the upper electrode.

After many hours of plasma operation, a copious deposit of particles on the lower electrode was obtained. Electron microscopy revealed that these particles were spherical and had a wide size distribution. Among them were spherical particles that had agglomerated in the plasma, forming string-shaped conglomerates.

[a]praburam@iowa.physics.uiowa.edu
[b]john-goree@uiowa.edu

 0734-2101/94/12(6)/3137/9/$1.00

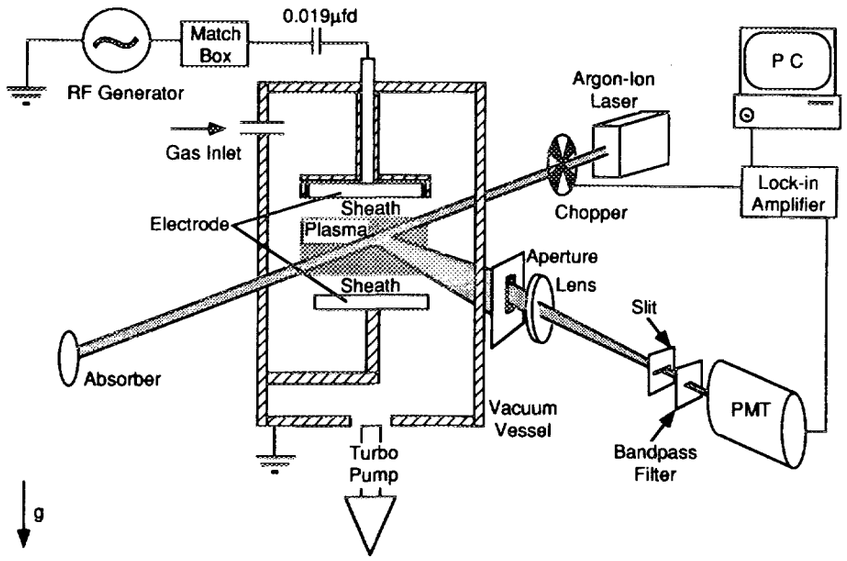

FIG. 1. Schematic of apparatus. The graphite electrodes are removable, for performing SEM on the particles that collect on them. The upper electrode is powered and water cooled, and it is fitted with a ground shield. The lower electrode is grounded. Laser light scattering is used to detect the particles suspended in the plasma. To provide a spatial profile, the transmitting and receiving optics are moved together on a vertical axis by a motorized linear translation stage (not shown). The slit views part of the laser beam, defining the spatial resolution.

II. EXPERIMENTAL TECHNIQUES

A. Apparatus

A capacitively coupled rf parallel-plate discharge was used to grow particles in our experiment. The apparatus, sketched in Fig. 1, includes a cylindrical aluminum vacuum vessel with a 32.4-cm i.d. and a 31.6-cm height. It was anodized black and fitted with Pyrex windows for making optical measurements. The parallel-plate electrodes were 6.2 cm in diameter and separated by 2 cm. Both electrodes were graphite disks, clamped to stainless-steel bases by a stainless-steel ring (Fig. 2). The electrodes were leveled with a precision circular bubble level. The upper electrode had a ground shield, was water cooled, and was powered by a 13.6-MHz rf signal from a function generator and a broadband amplifier (ar 200A15). The impedance was matched to the discharge by a pi-type matching network (Nye Viking MB-V-A) followed by a 0.019-μF coupling capacitor. The bottom electrode and the chamber walls were grounded.

Measurements of the rf voltage were made by a LeCroy 9400 digital oscilloscope, with Tektronix P6015 probe touching the vacuum feedthrough. The dc self-bias was measured as the midpoint between the wave form peaks, and it was typically -200 to -500 V, which is similar to other experiments.[5] The rf power reported below is calculated as the difference between forward and reverse powers, as measured with a Bird rf power meter inserted between the matching network and the rf amplifier. This measured power does not account for power losses in the matching network or feedthrough.

The system pressure was monitored by a convectron gauge (Granville–Phillips 275) and a baratron gauge (MKS

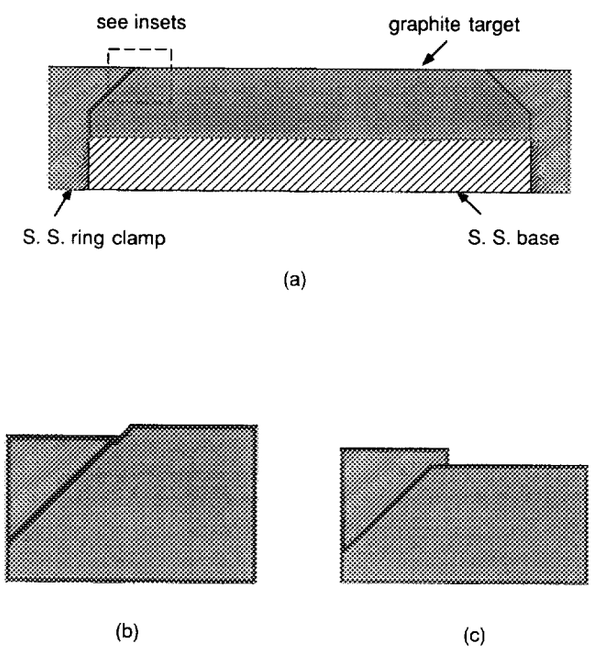

FIG. 2. (a) Topography of lower electrode. (b) Graphite surface projecting 0.5 mm above stainless-steel ring. (c) Graphite surface recessed 0.5 mm below stainless-steel ring. We found that (b) resulted in more particles falling to the lower electrode when the rf power was turned off, compared to (c).

122BA). Gases were admitted through inlets on the sidewall of the chamber and evacuated by a turbomolecular pump, providing a high gas flow rate of 141 sccm at 48 Pa.

We used spatially and temporally resolved LLS measurements to observe the growth and spatial distribution of particles in the plasma. An argon-ion laser beam (λ=488 nm) was directed through the center of the plasma, parallel to the electrode surfaces. The beam was vertically polarized, with a diameter of 1.4 mm. The 500-mW power did not perturb the particles. Scattered light was collected at 90° to the laser beam. The receiving optics consisted of an aperture followed by a lens, a slit, a bandpass filter and a photomultiplier tube (PMT), as shown in Fig. 1. The lens (150-mm focal length and 10-cm diam) focused the scattered light onto a horizontal slit, which was leveled parallel to the lower electrode. The slit was 80±10-μm wide and 15-mm long. The sampling region is the volume of the laser beam imaged by the slit; however, we found that the vertical spatial resolution is ~500 μm, rather than 80 μm as expected from the slit width. We were unable to determine the reason for this degradation in spatial resolution. Behind the slit, a 3-nm bandpass filter eliminated extraneous light. The PMT signal was detected by a lock-in amplifier, with a time constant of 100 ms. The lock-in was synchronized to a chopper, which modulated the incident laser light at 600 Hz.

The scattered light signal indicates the presence of particles. We made no effort to obtain values for the particle size or number density from the LLS. Instead, we used the data only to study the spatial distribution of the particles. To measure the vertical profile of the particulate clouds, the transmitting and receiving optics were moved together, at 0.027 cm/s, on a vertical axis. The lock-in signal and the position were recorded at a 10-Hz sampling rate with a 12-bit digitizer.

Scanning electron microscopy (SEM) was performed to characterize the particle size and morphology. After the plasma was turned off, the lower electrode was removed from the vacuum chamber, and the particles were left undisturbed on the graphite electrode. The electrode was inserted, with the particles intact, into the SEM. We imaged the electrode surface using an Hitachi S-4000 SEM, with a beam voltage of 4–5 kV, which was low enough not to disturb the particles.

III. RESULTS

A. Conditions leading to electrode contamination

We found that the topography of the lower electrode surface affects whether particles fall to the lower electrode. This is consistent with the observations of other experimenters.[15] As shown in Fig. 2, the graphite target was clamped to a stainless-steel base by a stainless-steel ring. Two configurations were tested: the graphite electrode was either projecting 0.5 mm [Fig. 2(b)] or recessed 0.5 mm [Fig. 2(c)], with respect to the stainless-steel ring. We found that the projecting configuration of Fig. 2(b) resulted in a greater deposit of particles on the electrode.

Particles that escape the trapping region in the radial direction will never contaminate the electrode. A dust-free discharge usually has a plasma potential that is positive in the plasma center, so that a single particle with a negative charge would not be expected to escape in the radial direction. However, our visual observations revealed that in the lowest layer, a constant stream of particles escaped the plasma in the radial direction. These particles were large enough to image individually, and were therefore probably much larger than a micron. We do not know whether smaller particles also escaped this way. We were able to see this process of radial escape through a window, because the laser beam illuminated a chord parallel to the electrode surfaces. We are uncertain whether this escape is due to an inverted electric potential profile in the radial direction, or due to a drag force.

The mode of plasma shut off was also a deciding factor for particle collection on the lower electrode. When the rf power was turned off before the gas, particles fell to the electrode. On the other hand, when the gas was shut off first, particles were seen escaping in a radial direction from the interelectrode region even before the plasma extinguished.

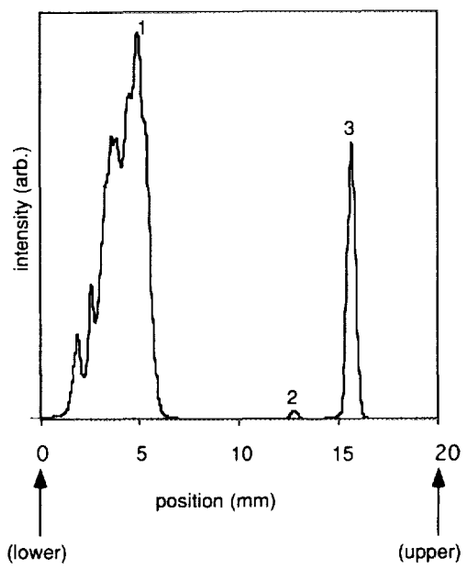

FIG. 3. Spatial distribution of LLS signal from particles levitated within the discharge. The LLS intensity increases with increasing particle number density and size. Feature 1 is a multilayered dust cloud near the sheath edge, above the lower electrode. Visual observations indicate that the layers are thinner than shown here; they are actually distinct and do not overlap. Feature 3 is a thin dust layer near the upper sheath edge, while feature 2 is a layer within the glow region. The discharge parameters are 6.7% SF_6 diluted by argon, total pressure 48 Pa (360 mTorr), rf power P_{rf}=140 W, and dc self-bias V_{dc}=−390 V.

B. Spatial distribution

The spatially resolved LLS measurements show that particles form clouds that are stratified in multiple layers. We use the term "layer" to describe a sharp formation with a thickness on the order of 1 mm, and the term "cloud" to mean a localized group of one or more layers.

Figure 3 shows the scattered light signal as a function of

position for a 48 Pa (360 mTorr) plasma of 6.7% SF_6 diluted by argon. The dust clouds in Fig. 3 are labeled as follows. Feature 1 is a multilayered cloud near the sheath edge above the lower electrode. The overlapping peaks in the lower cloud indicate that the particles are stratified in multiple layers. Feature 2 is a thin dust layer suspended in the glow region and feature 3 reveals a dust layer near the upper sheath edge.

Visual observations revealed that layers were even thinner than shown in Fig. 3. The thinnest layer recorded by the LLS profile was 0.5 mm, but to the naked eye it appeared razor-thin; noticeably sharper than 0.5 mm. (Our LLS apparatus apparently has a vertical spatial resolution of 0.5 mm.) The peaks in the lower cloud were seen as distinct layers with clear voids between them. Although the peaks appear to overlap in the LLS profile of Fig. 3, this is only due to the instrumental resolution.

By simple visual observations, we verified that the different layers separated particles according to size. Massive particles were seen suspended in the lower layers, while particles too small to identify individually were in the upper layers. Each layer appeared to contain particles of a narrow size distribution. Apparently, a particle of a given size finds an equilibrium height where the net force is zero. It is expected that this equilibrium height depends on particle size, as discussed in Sec. IV. The layer stratification is sensitive to discharge parameters, such as rf power, pressure, and electrode separation, presumably because the plasma potential profile, which is responsible for particles' distribution, is modified by a change in discharge parameters.

C. Parametric studies

Temporally and spatially resolved LLS profiles were recorded for various discharge parameters. The results are shown in Figs. 4–10, and the parameters and observations for these figures are summarized in Table I. We found that the particle clouds grew to a detectable level within minutes, and they continued to evolve during several hours of continuous plasma operation. Under most of the conditions we studied, a cloud at a given height grew until it collapsed, and then sometimes grew and collapsed again. In the parametric studies described below, we first examined pure argon plasmas. Then we repeated some of the tests with a mixture of SF_6 and argon.

1. Growth and collapse

For a pure argon plasma, Fig. 4 shows the temporal development of the dust layers. Only one cloud was observed, near the sheath boundary above the lower electrode. This cloud consisted of two layers during the first half-hour. After 60 min, the largest peak attained its maximum level and then collapsed into two overlapping peaks. Then, after 240 min, the dust cloud diminished.

The collapse is a rapid process. We made a number of efforts to record the spatial distribution during the collapse, and this was always unsuccessful, due to the speed of the collapse. We were only able to record the profiles before and after. The reason for the collapse is not understood.

2. Pressure dependence

We found that increasing the argon pressure yields faster growth before the collapse. This result is in agreement with Selwyn *et al.*,[5] who observed greater light scattering at higher gas pressures. Our results offer greater detail, because we report the temporal dependence for a longer duration.

To see how the peaks grow more rapidly at a higher pressure, examine the peaks at 20 and 30 min in Figs. 4 and 5. The pressure was 48 Pa for Fig. 5, compared to 29 Pa for Fig. 4, while the other parameters were the same. In both the cases, particles form in clouds near the lower electrode, but at higher pressure their growth is faster.

Higher pressure also leads to an earlier collapse. In Fig. 5 the peak collapsed at 30 min and again at 60 min, while in Fig. 4 there was only one collapse, at 120 min. We also found that higher pressure leads to a broader peak. The FWHM of the peak at 60 min in Fig. 5 is 0.8 mm, compared to 0.5 mm in Fig. 4.

3. rf power dependence

For a pure argon plasma, higher rf power results in fewer layers, and in faster growth followed by collapse. Figure 6 shows the profiles at higher rf power (120 W) compared to 55 W for Fig. 7. The other parameters were the same (except for the dc self-bias, which increases with rf power).

Higher rf power leads to a much faster start for the particle growth. After only 5 min, there was a very substantial light scattering signal. The dust cloud at this early time extended throughout the glow region (feature 4 in Fig. 6) and even into the sheath dark space (feature 5).

For the high rf-power case (Fig. 6) visual observation showed that the particle cloud extended laterally 3–4 cm beyond the interelectrode region, during the first few minutes of plasma operation. Apparently the particle trap extended in the radial direction far beyond the electrode edge. (This observation was surprising, so we repeated the experiment several weeks later and verified that it was repeatable.) This condition did not persist long. After the first few minutes, particles were observed only in the interelectrode region.

After several hours of operation, the higher power discharge contained a smaller number of dust layers, with less light scattering. At 360 min, Fig. 6 shows a diminished dust cloud with only two layers near the lower electrode. In contrast, Fig. 7 exhibits multiple layers with stronger light scattering at this time. Additionally, we note that at higher power, the peaks suffered several collapses. At lower power, there was no collapse at all during 420 min of operation.

4. Electrode separation

Increasing the electrode separation from 2.0 to 2.5 cm results in slower growth and fewer stratified layers. Figures 7 and 8 have nearly the same parameters, except that in Fig. 8 the electrode separation was increased to 2.5 cm. Comparing the peaks in Figs. 7 and 8 at 60 min, we find that a larger electrode separation leads to slower initial growth during the first hour of operation. Later, at 360 min, the profile in Fig. 8 shows only two stratified layers near the lower electrode,

TABLE I. Parameters and observations for Figs. 4–10. The first column indicates whether the peaks collapse, and if so, whether this happens in a cloud near the upper or lower electrode. The vertical scales on figures with the same PMT bias can be compared.

	Parameters						Results		
		Pressure (Pa)				Number of dust cloud layers			
Fig.	Electrode separation (cm)	Argon	SF_6	Power (W)	dc self-bias (V)	PMT bias	Lower	Middle	Upper	Peak collapse
4	2.0	29		105	−490	A	3	0	0	Lower
5	2.0	48		105	−390	A	3	0	0	Lower
6	2.0	55		120	−476	B	3	0	0	Lower
7	2.0	55		55	−315	B	>3	0	0	No
8	2.5	55		60	−344	B	2	0	0	No
9	2.0	48	3.25	100	−160	A	>3	1	1	Lower and upper
10	2.0	48	3.25	140	−323	A	>5	1	1	Lower and upper

while Fig. 7 has multiple peaks. In both the cases, the rf power was low, and there was no peak collapse.

D. Negative ions (SF_6)

To observe the sensitivity of the particle formation to the gas composition, we added 6.7% SF_6 to the argon. SF_6 is a gas commonly used in plasma etching, where particle growth is a worrisome source of contamination.[5] After processing silicon wafers with SF_6/Ar, Smadi *et al.*[16] detected particle contaminants on the wafers. They reported the particle contamination counts for various plasma parameters. Electrons attach easily to SF_6, resulting in a population of negative ions in the plasma. The plasma potential profile, which is presumably responsible for particle growth and distribution, is altered by the negative ions. This is indicated by the dc self-bias (see Table I), which was diminished by adding SF_6.

We found that adding SF_6 did not change the growth rate of the clouds much, but it did lead to a much larger number of dust layers. Most significantly, it led to three clouds, rather than just one at the lower electrode, as with pure argon. There were clouds at both the upper and lower electrodes, plus a cloud in the central glow region. The additional two clouds are labeled as features 2 and 3 in Fig. 9. We presume that the additional clouds are due to a plasma potential that is altered by the negative ion space charge, although we did not measure the plasma potential to verify this explanation.

When SF_6 was used, all the clouds did not grow at the same rate. In Fig. 9, the upper cloud (feature 3) grows faster and collapses more frequently than the corresponding lower cloud (feature 1). Peaks in the lower cloud collapse more frequently than in pure argon (Fig. 5). The middle cloud (feature 2) grows slowly and saturates without any collapse. All three clouds in Fig. 9 have comparable peak widths. At 180 min, the FWHM of the lower, middle, and upper peaks is 0.57, 0.5, and 0.58 mm, respectively.

X-ray spectral analysis was performed on the particles grown in the 6.7% SF_6 plasma. This revealed traces of Fe and Ni, apparently due to fluorine etching of the stainless-steel ring. We presume that the particles were mainly made of carbon from the graphite targets, but we were unable to verify this using our x-ray analysis setup, because it could not detect elements with low atomic numbers.

We tried two different rf power levels using SF_6. As with pure argon, we found that a higher rf power results in faster growth and frequent collapse. Unlike pure argon, a higher rf power led to more, rather than fewer, stratified layers. Figures 9 and 10 show LLS profiles using SF_6 with similar parameters, except that Fig. 10 is for a higher rf power of 140 W. Comparing the profiles at 30 min, one can see that higher power leads to faster growth in both upper and lower clouds. Both the upper and lower peaks in Fig. 10 grow faster and collapse more frequently than in Fig. 9. The middle peak, on the other hand, behaves the same at the two different rf power levels.

We also tried varying the SF_6 concentration. This had a significant effect not only in the particles' spatial distribution, but also in determining whether particles grew at all. In this test, we varied the SF_6 concentration in a 120-W argon plasma with a constant total pressure of 55 Pa. The particle growth was maximized at 6% SF_6, diminished at 4.8% and 6.7% SF_6, and was eliminated entirely above 7% SF_6. The

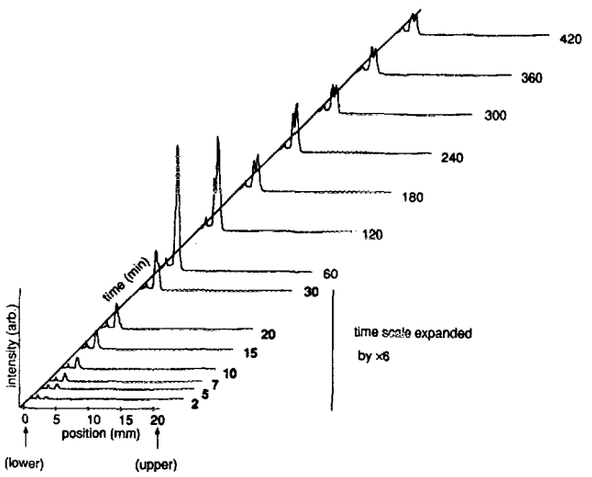

FIG. 4. Temporally and spatially resolved profiles of LLS scattering in a pure argon discharge. Particle layers are found only near the lower electrode. Note that layers grow and then collapse into more stratified layers. The plasma parameters are argon pressure=29 Pa, P_{rf}=105 W, and V_{dc}=−490 V. The vertical scale is the same as in Figs. 5 and 9.

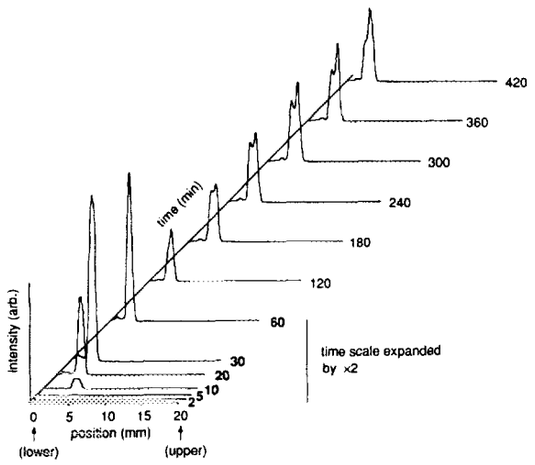

FIG. 5. Profile as in Fig. 4, but with a higher argon pressure of 48 Pa. A higher pressure yields a faster growth of dust layers. The other parameters are $P_{rf}=100$ W and $V_{dc}=-390$ V.

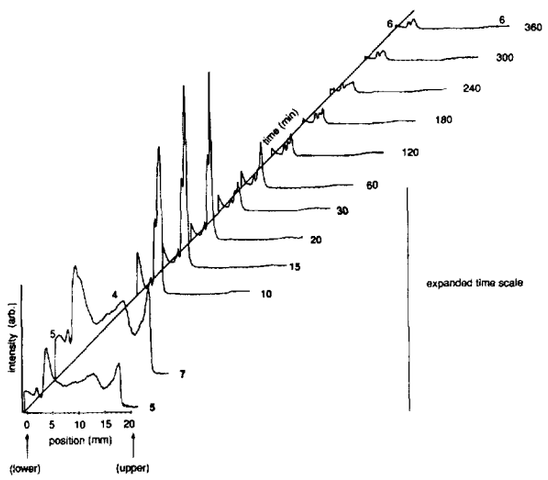

FIG. 6. Profile at higher pressure and higher rf power. Initially, particles grow throughout the glow region (feature 4) and are found even in the sheath dark space region (feature 5). Later, after 180 min, dust clouds diminish and there are fewer layers. Features 6 are artifacts of scattered light from electrodes, windows and other surfaces; they are weaker than feature 4, which is due to dust particles. Plasma parameters are argon pressure=55 Pa, $P_{rf}=120$ W, and $V_{dc}=-470$ V. The vertical scale is the same as in Fig. 8.

lack of particle growth at high SF_6 concentrations is presumably due to a lower plasma potential and hence a shallower trap.

E. Thermophoretic effect

Other researchers have reported that particles are sensitive to thermophoretic forces, established by temperature gradients in the neutral gas. Jellum *et al.*[7] demonstrated that carbon particles suspended in an argon discharge move away from a heated electrode and towards a cooled electrode. Their apparatus was similar to ours, except that they used a lower gas flow of 5–10 sccm through a showerhead electrode.

We attempted to observe the thermophoretic effect on carbon particles in our argon discharge, but we saw no effect. In this test, we heated and then cooled our powered electrode by controlling the cooling water temperature. This was done using a closed-cycle water heater/chiller. The upper electrode's temperature was calibrated for various water temperatures before the discharge was turned on, using a thermocouple fixed to the surface of the top electrode. (We note that this method of calibrating the electrode temperature does not account for any heating due to plasma exposure.) The temperature of the lower (grounded) electrode was uncontrolled.

A 30 Pa argon discharge was started, with $P_{rf}=100$ W and $V_{dc}=-400$ V. Particles grew in clouds, as usual for our experiments. After 280 min, when the dust clouds had reached a steady state, the test began. The water was initially chilled, and then heated gradually. The corresponding electrode temperature ranged from 17 °C at the start to 36 °C at the end.

The variation of 19 °C in the electrode temperature caused no measurable displacement of the particle layers in our test. This result suggests that the thermophoretic force is not always significant. In contrast, Jellum *et al.*[7] used a similar procedure and the conditions are generally similar, but observed a significant movement of particle to the cooled electrode. The only significant differences between their experiment and ours, to the best of our knowledge, was their use of a lower gas flow rate and a gas inlet in the upper electrode. Both of these factors might promote a more significant gas temperature gradient in the interelectrode region. Using a lower flow rate might reduce the heat loss by pro-

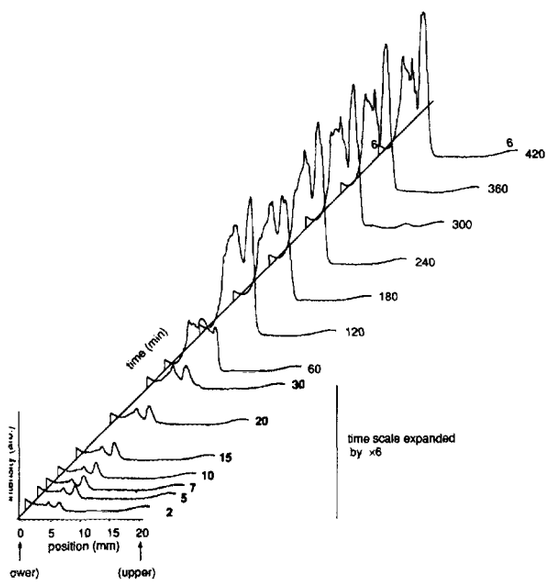

FIG. 7. Profile as in Fig. 6, but with lower rf power. Lower power yields slower growth, no collapse, and more layers. As in Fig. 5, feature 6 is an artifact. Parameters are argon pressure=55 Pa, $P_{rf}=55$ W, and $V_{dc}=-315$ V. The vertical scale is expanded by two times compared to Fig. 6.

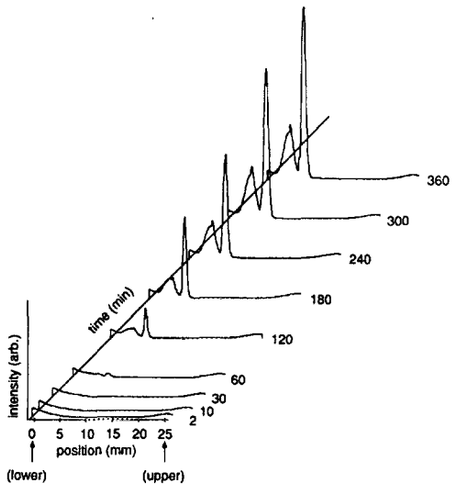

FIG. 8. Profile as in Fig. 7, but with an increased electrode separation of 2.5 cm. Increasing the electrode spacing results in slower growth and fewer layers. Parameters are argon pressure=55 Pa, P_{rf}=60 W, and V_{dc}=−340 V.

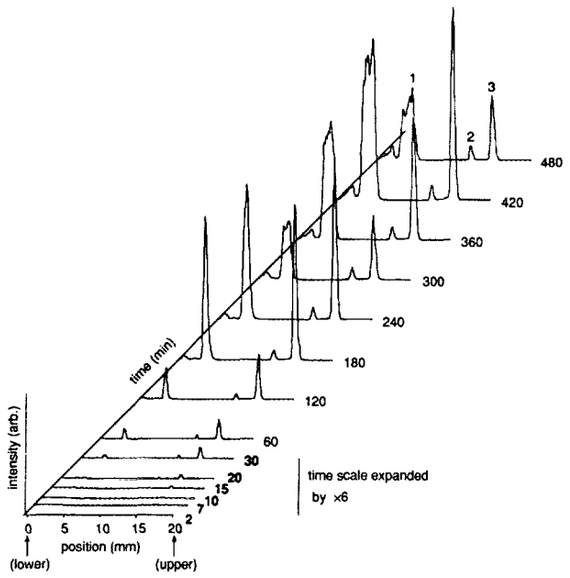

FIG. 9. Profile as in Fig. 5, but with an addition of 6.7% SF_6. Adding SF_6 yields additional peaks, one near the upper electrode (feature 3) and another in the glow region (feature 2). The lower and upper peaks collapse frequently. The lower cloud (feature 1) is stratified into many layers. Parameters are total pressure=48 Pa, P_{rf}=100 W, and V_{dc}=−160 V.

longing the time a given gas atom is present in the interelectrode region. Flowing the gas through the temperature-controlled upper electrode might heat or cool it more effectively than in our setup, where the gas inlet was on a side flange.

F. Gas flow

To observe the sensitivity of particle growth to gas flow, we repeated an experiment with no gas flow. The vacuum system was evacuated to the base pressure and then sealed. Then argon was admitted to a pressure of 55 Pa. A discharge was operated with P_{rf}=60 W and V_{dc}=−336 V.

Particle growth was reduced considerably without gas flow. LLS measurements showed very slow growth during 30 min of discharge operation. We have no explanation for this result, which is contrary to the results reported by other experimenters. Selwyn *et al.*[5] used an etching plasma, and found more scattering at low gas flow rates. Ganguly *et al.*[11] performed an experiment with argon sputtering of graphite targets, and it was similar to ours except for their use of a much lower frequency and a glass tube instead of a metal vacuum vessel. They observed prolific particle growth with no gas flow.

G. dc plasmas

While most experiments of particles grown in plasmas were done using rf plasmas, there are reports of particle growth in other devices as well. For example, Jellum and Graves[4] demonstrated particle growth in a dc sputtering discharge with argon gas and an aluminum target. Particles grew in this device using either dc or rf power.

We tried dc power in our device, but we found that particles did not grow. One might expect a slower growth rate in a dc discharge due to a lower plasma density, so we operated the discharge for a long duration of 290 min. Our tests were done in a 55-Pa dc discharge with various applied voltages (typically 440 V) with the upper electrode acting as the cathode. Neither a pure argon discharge nor a discharge with 6.7% SF_6 produced any particles. Both the LLS signal and visual observation gave negative indications. These results appear contrary to those of Jellum and Graves,[4] whose setup was similar to ours, except for an aluminum target instead of graphite.

In another comparison of dc and rf discharges, we introduced micron-size aluminum oxide powder into a plasma with stainless-steel electrodes, and we obtained similar results. The rf discharge easily levitated the particles, while the dc plasma did not. These results lead us to conclude that dc plasmas do not levitate particles as easily as rf discharges.

H. Particle size and morphology

The carbon particles collected on our lower electrode had a wide size distribution, as shown in the electron micrograph in Fig. 11. The size ranges from 10 nm to over 1 μm. These particles were grown over the course of 7 h of plasma operation. The experiment was the same one that yielded the data of Fig. 6.

We presume that the smaller particles are formed later than the larger ones. Particles can begin growing from the sputtered flux of carbon atoms at any time during the discharge. Some of the larger particles may have fallen to the electrode before the rf power was turned off, because they were too large to levitate.

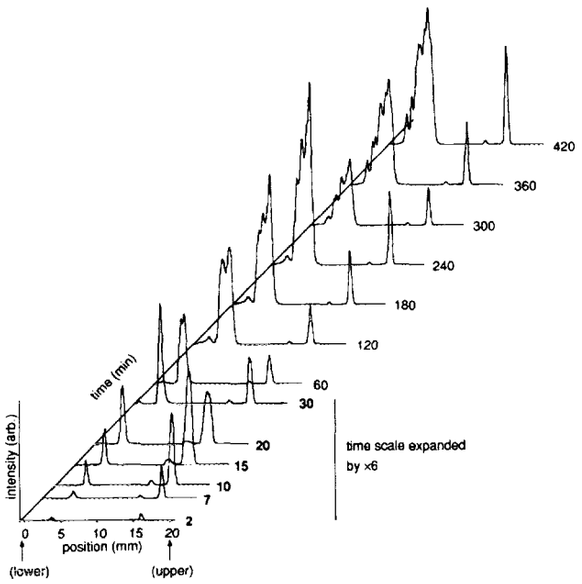

FIG. 10. Profile as in Fig. 9, but with higher rf power. Higher power permits faster growth and more stratified layers. Parameters are total pressure=48 Pa, P_{rf}=140 W, and V_{dc}=−390 V. The vertical scale is compressed by five times compared to Fig. 6.

A cauliflowerlike surface is evident in the particles shown in Fig. 11. Cauliflower structures were also observed by Selwyn *et al.*[5] and Ganguly *et al.*,[11] who explained it as the result of an internal columnar structure, similar to the columnar morphology found in thin films. Columns develop in thin films grown on a substrate that is less than half the melting temperature of the sputtered material.[17]

We observed coagulated particles as shown in Fig. 11. Dozens of spherical particulates stuck together to form a string-shaped cluster. The particles that have stuck together appear to have a narrow size distribution. We believe that these particles coagulated while they were suspended in the plasma. All other possibilities can be ruled out. We took care not to disturb the particles after they fell to the electrode, and we transferred the entire electrode from the plasma chamber to the SEM. For this reason we are certain that *ex situ* handling did not lead to the coagulation. Another possibility is that the clusters formed as particles landed on top of one another on the electrode. This seems unlikely, based on the arrangement of the spheres in the coagulated structure in Fig. 11.

IV. DISCUSSION

The particles in the plasma are confined radially and axially. The radial confinement is due to the electrical force, while the axial confinement is due to a sum of electrical, collisional and gravitational forces. The particles are suspended at a position where the net force acting on them is zero. Because of the neutral gas drag, they lose their kinetic energy and thermalize with the gas after only few seconds.

The various forces scale with particle radius a, electric field E, and ion drift velocity V_i as follows:

electrical $F_e \propto aE$;
ion drag $F_i \propto a^2 V_i$;
neutral drag $F_n \propto a^2$;
thermophoretic $F_t \propto a^2$;
gravitational $F_g \propto a^3$.

The forces do not scale similarly with particle size, and the electric field and ion velocity in a plasma are nonuniform. For these two reasons, the position of zero net force depends on particle size. Thus, particles are separated at different heights according to their size. This stratification by particle size has been verified in a theoretical study by Nitter *et al.*, who included the electrical and gravitational forces, but not ion drag.[18]

V. SUMMARY

Particles grow due to sputtering in an argon rf discharge with graphite electrodes. Laser light scattering measurements indicate that the particles are levitated in multiple layers. These layers are grouped into clouds. In a pure argon plasma, there is one cloud near the sheath edge above the lower electrode, while adding SF_6 results in additional particle clouds near the upper electrode and in the glow region.

The layers are revealed as peaks in the vertical profiles of the LLS signal. Under most conditions studied, the lower peak undergoes a rapid collapse after about 1 h of plasma operation. After collapsing, the peak may reappear. Conditions favorable for collapse are high rf power, high gas pressure, and addition of SF_6. In a pure argon plasma, collapse was not observed for lower rf power or increased electrode separation. The cause of the collapse is unknown. The growth rate of the dust clouds is slowest at low rf power, low gas pressure, and an increased electrode separation. We did not observe particle growth when the plasma was operated with dc rather than rf power.

The different layers appear to separate particles according to size. Particles of different sizes levitate at different heights due to the variation of the electric and ion velocity fields in the plasma, and the different scalings of the electric, ion drag, and gravitational forces on particle size. We observed

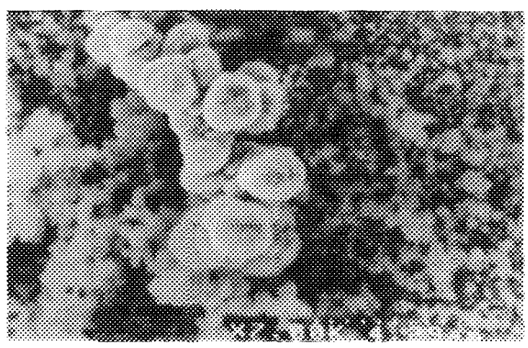

FIG. 11. SEM images of carbon particles grown after 7 h exposure to a 55-Pa argon plasma. The particles have a wide size distribution and a cauliflowerlike surface texture. Note the larger particles that have stuck together forming a coagulated string.

no displacement of the layers due to the thermophoretic force when we varied the upper electrode temperature by 19 °C.

Particles fell to the lower electrode after the discharge was shut off. They have a wide size distribution and a cauliflower-like surface. Some larger particles were coagulated.

ACKNOWLEDGMENTS

The authors thank B. Ganguly for helpful discussions. This work was supported by NSF ECS-92-15882, NASA Origins of the Solar System Program NAGW-3126, and NASA Microgravity Science and Applications Division NAG8-292.

[1]K. G. Spears, T. J. Robinson, and R. M. Roth, IEEE Trans. Plasma Sci. **PS-14**, 179 (1986).
[2]M. Shiratani, T. Fukuzawa, and Y. Watanabe, IEEE Trans. Plasma Sci. **PS-22**, 103 (1994).
[3]G. S. Selwyn, J. E. Heidenreich, and K. L. Haller, Appl. Phys. Lett. **57**, 1876 (1990).
[4]G. M. Jellum and D. B. Graves, J. Appl. Phys. **67**, 6490 (1990).
[5]G. S. Selwyn, J. Singh, and R. S. Bennett, J. Vac. Sci. Technol. A **7**, 2758 (1989).
[6]H. M. Anderson, R. Jairath, and J. L. Mock, J. Appl. Phys. **67**, 3999 (1990).
[7]G. M. Jellum, J. E. Daugherty, and D. B. Graves, J. Appl. Phys. **69**, 6923 (1991).
[8]Ph. Belenguer, J. Ph. Blondeau, L. Boufendi, M. Toogood, A. Plain, A. Bouchoule, C. Laure, and J. P. Boeuf, Phys. Rev. A **46**, 7923 (1992).
[9]W. Böhme, W. E. Köhler, M. Römheld, S. Veprek, and R. J. Seeböck, IEEE Trans. Plasma Sci. **PS-22**, 110 (1994).
[10]A. Bouchoule, A. Plain, L. Boufendi, J. Ph. Blondeau, and C. Laure, J. Appl. Phys. **70**, 1991 (1991).
[11]B. Ganguly, A. Garscadden, J. Williams, and P. Haaland, J. Vac. Sci. Technol. A **11**, 1119 (1993).
[12]C. K. Goertz, Rev. Geophys. **27**, 271 (1989).
[13]H. Hahn and R. S. Averback, J. Appl. Phys. **67**, 1113 (1990).
[14]G. M. Chow, R. L. Holtz, A. Pattnaik, A. S. Edelstein, T. E. Schlesinger, and R. C. Cammarata, Appl. Phys. Lett. **56**, 1853 (1990).
[15]G. S. Selwyn, J. Vac. Sci. Technol. B **9**, 3487 (1991).
[16]M. M. Smadi, G. Y. Kong, R. N. Carlile, and S. E. Beck, J. Vac. Sci. Technol. B **10**, 30 (1992).
[17]R. C. Ross and R. Messier, J. Appl. Phys. **52**, 5329 (1981).
[18]T. Nitter, T. K. Aslaksen, F. Melandsø, and O. Havnes, IEEE Trans. Plasma Sci. **PS-22**, 159 (1994).